



Nuclear Materials  
Modeling Lab.



# Effect of Al Concentration on Microstructural Evolution of Fe-Cr-Al System: A Phase-field Approach

Jeonghwan Lee, Kunok Chang\*  
Department of Nuclear Engineering, KyungHee University



# Contents

---

**Research Motivation**

---

**Simulation Method**

---

**Results and Future work**

---

**Conclusions**

---

**Acknowledgement**

---

## Background

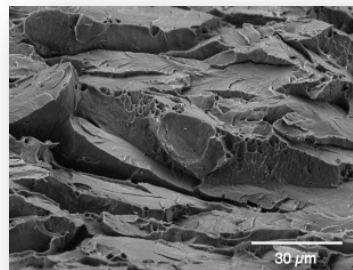


### Fe-Cr-Al alloy

- Fe-Cr alloy is widely used in various fields.
- The addition of Al to Fe-Cr alloy has been considered as an effective method to improve the mechanical properties.



Kanthal APM FeCrAl alloy tube



SEM micrograph of the fracture surface of 21Cr-5Al (Jesper Ejenstam et al).

### Strength

- Excellent corrosion resistance and high temperature strength.
- Excellent radiation tolerance and mechanical properties.

### Weakness

- The formation of  $\alpha'$  phase, which generates embrittlement in the system.

## Background



### $\alpha'$ phase precipitation

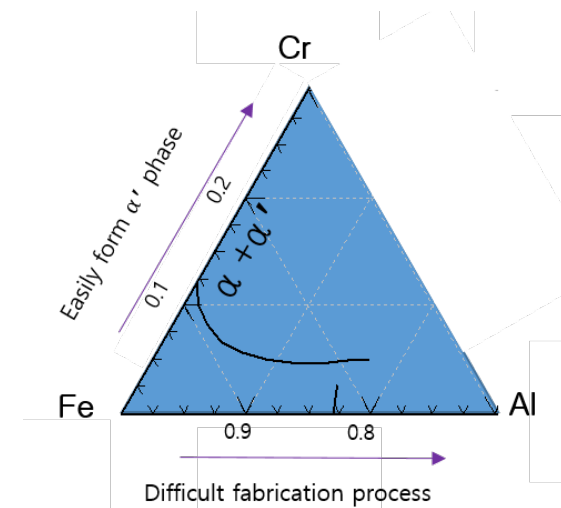
- Cr rich phase.
- Degrade integrity of materials.

### Phase-field model

- Phase-field model is thermodynamic and kinetics based model
- Quantitative modeling of phase transformations and microstructure evolutions.

### Calculation of phase diagram (CALPHAD) method

- CALPHAD method is a methodology to predict the system.
- It is used to simulate behavior of multicomponent phase.



## Simulation Method

### CALPHAD Combined Phase-field modeling in ternary system

- Total free energy of Fe-Cr-Al system and Cahn-Hilliard equation.

$$F(r, t) = \int_V \left\{ \frac{1}{V_m} \left[ G(c_{\text{Fe}}, c_{\text{Cr}}, c_{\text{Al}}) + \frac{1}{2} \kappa (\nabla c_{\text{Fe}})^2 + \frac{1}{2} \kappa (\nabla c_{\text{Cr}})^2 + \frac{1}{2} \kappa (\nabla c_{\text{Al}})^2 \right] \right\} dV$$

$c_i$  : Concentration of  $i$  component.

- Chemical free energy in ternary system.

$$G(c_{\text{Fe}}, c_{\text{Cr}}, c_{\text{Al}}) = c_{\text{Fe}} G_{\text{Fe}}^0 + c_{\text{Cr}} G_{\text{Cr}}^0 + c_{\text{Al}} G_{\text{Al}}^0 + L_{\text{FeCr}} c_{\text{Fe}} c_{\text{Cr}} + L_{\text{CrAl}} c_{\text{Cr}} c_{\text{Al}} + L_{\text{FeAl}} c_{\text{Fe}} c_{\text{Al}} + RT [c_{\text{Fe}} \ln(c_{\text{Fe}}) + c_{\text{Cr}} \ln(c_{\text{Cr}}) + c_{\text{Al}} \ln(c_{\text{Al}})]$$

- Onsager type mobility.

$$M_{\text{Cr,Cr}}(c_{\text{Fe}}, c_{\text{Cr}}, c_{\text{Al}}) = c_{\text{Cr}} [(1 - c_{\text{Cr}})^2 M_{\text{Cr}} + c_{\text{Cr}} c_{\text{Al}} M_{\text{Al}} + c_{\text{Cr}} c_{\text{Fe}} M_{\text{Fe}}]$$

$$M_{\text{Al,Al}}(c_{\text{Fe}}, c_{\text{Cr}}, c_{\text{Al}}) = c_{\text{Al}} [(1 - c_{\text{Al}})^2 M_{\text{Al}} + c_{\text{Cr}} c_{\text{Al}} M_{\text{Cr}} + c_{\text{Al}} c_{\text{Fe}} M_{\text{Fe}}]$$

$$M_{\text{Cr,Al}}(c_{\text{Fe}}, c_{\text{Cr}}, c_{\text{Al}}) = M_{\text{Al,Cr}} = c_{\text{Cr}} c_{\text{Al}} [c_{\text{Fe}} M_{\text{Fe}} - (1 - c_{\text{Cr}}) M_{\text{Cr}} - (1 - c_{\text{Al}}) M_{\text{Al}}]$$

## Simulation Method

### □ Semi-implicit Fourier spectral method □ Constraint

$$\frac{\partial c_{Cr}(r,t)}{\partial t} = \nabla \cdot \left[ M_{Cr,Cr} \nabla \left( \frac{\delta F}{\delta c_{Cr}} \right) + M_{Cr,Al} \nabla \left( \frac{\delta F}{\delta c_{Al}} \right) \right]$$

$$\frac{\partial c_{Al}(r,t)}{\partial t} = \nabla \cdot \left[ M_{Al,Al} \nabla \left( \frac{\delta F}{\delta c_{Al}} \right) + M_{Al,Cr} \nabla \left( \frac{\delta F}{\delta c_{Cr}} \right) \right]$$

- 4<sup>th</sup> rank differential equation.  $\nabla^4$
- The equation has severe time constraint.  $\Delta t \kappa k^4$
- Concentration dependence of mobility.  $M_{i,j}(c_{Fe}, c_{Cr}, c_{Al})$

### □ Semi-implicit Fourier spectral scheme

$$\tilde{c}_A^{n+1}(k, t) = \tilde{c}_A^n(k, t) + \frac{\Delta t i k}{(1 + S_A \Delta t \kappa k^4)} \cdot \{ M_{A,A} \times [i k' \left( \left\{ \frac{\partial F}{\partial c_A} \right\}_{k'}^n + 2 \kappa k'^2 \tilde{c}_A^n + \kappa k'^2 \tilde{c}_B^n \right)]_r + M_{A,B} \times [i k' \left( \left\{ \frac{\partial F}{\partial c_B} \right\}_{k'}^n + 2 \kappa k'^2 \tilde{c}_B^n + \kappa k'^2 \tilde{c}_A^n \right)]_r \}_k$$

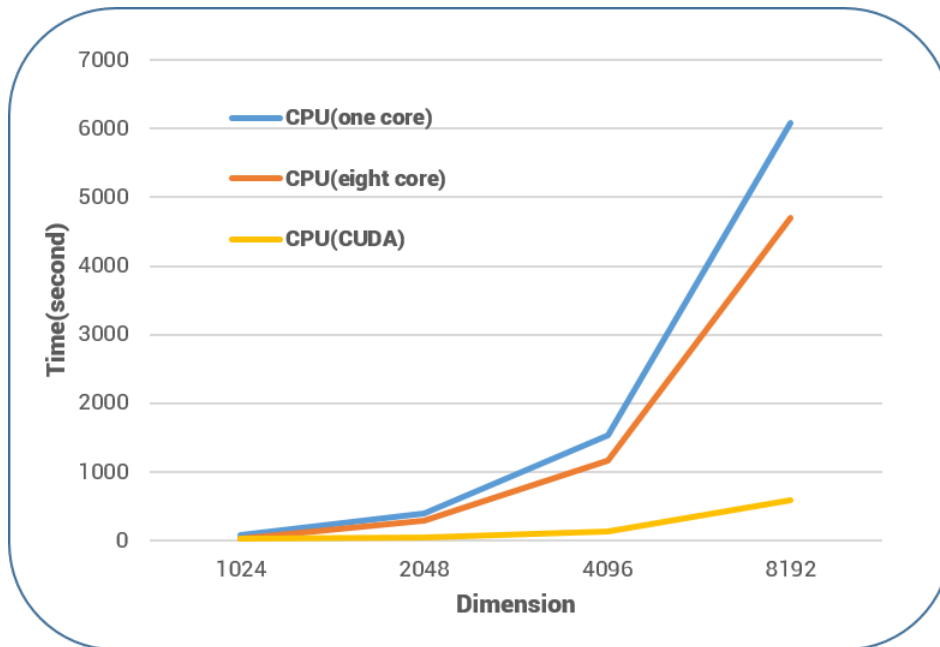
- We solved Cr and Al concentration over time, respectively.

## Simulation Method



### GPU parallel computing scheme

### Performance benchmark



### Strength

- The GPU calculation is powerful when performing 3D large scale simulations.
- It costs less compared to building a CPU cluster.

### Constraint

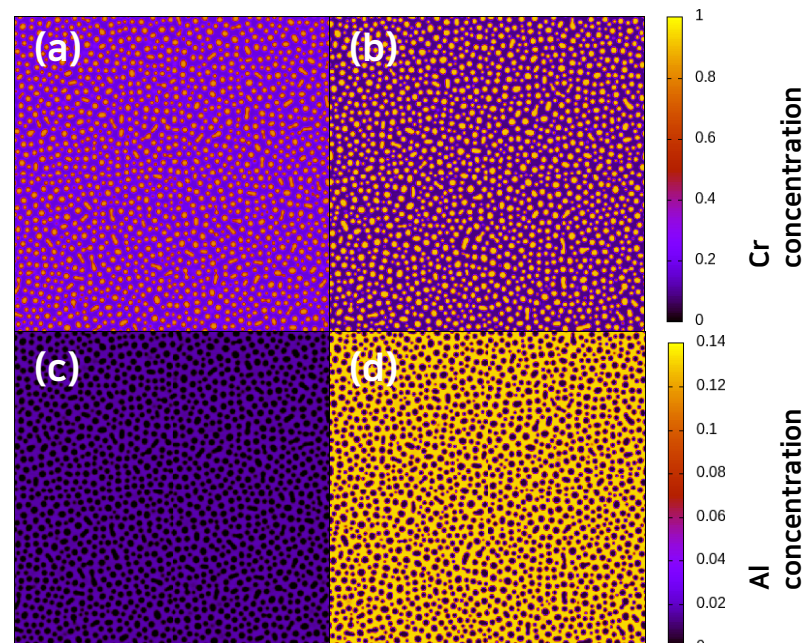
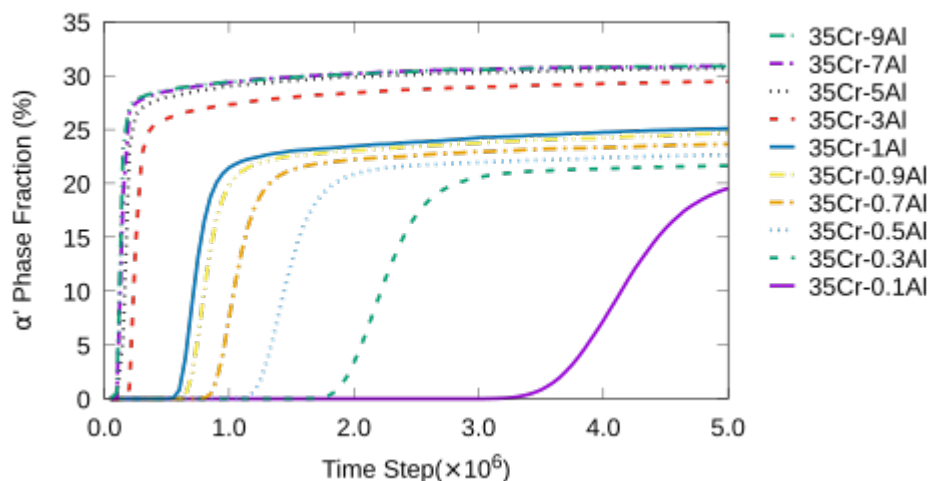
- The GPU calculation is difficult for memory intensive calculations.

## Results

### 2D simulation result

As the Al concentration increase

- The difference of Cr and Al concentration between the  $\alpha'$  (Cr-riched) phase and the  $\alpha$  (Cr-depleted) phase increase.
- The  $\alpha'$  phase fraction increase.



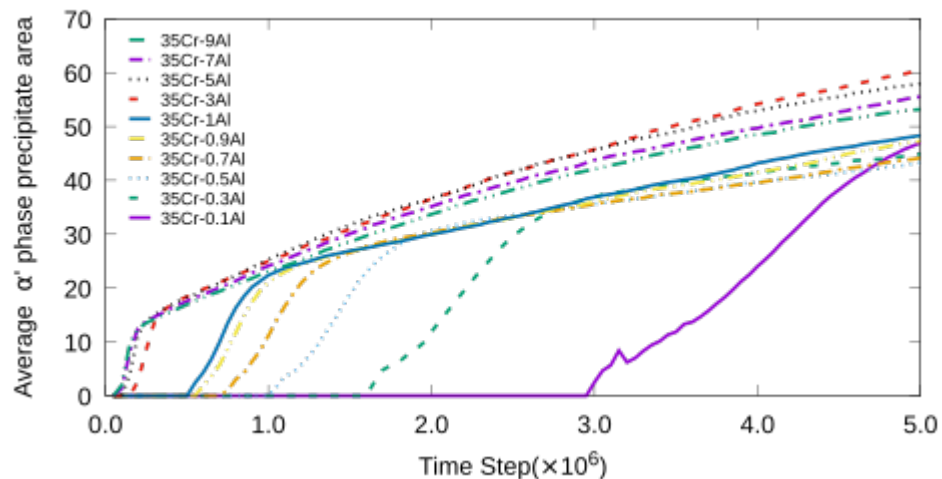
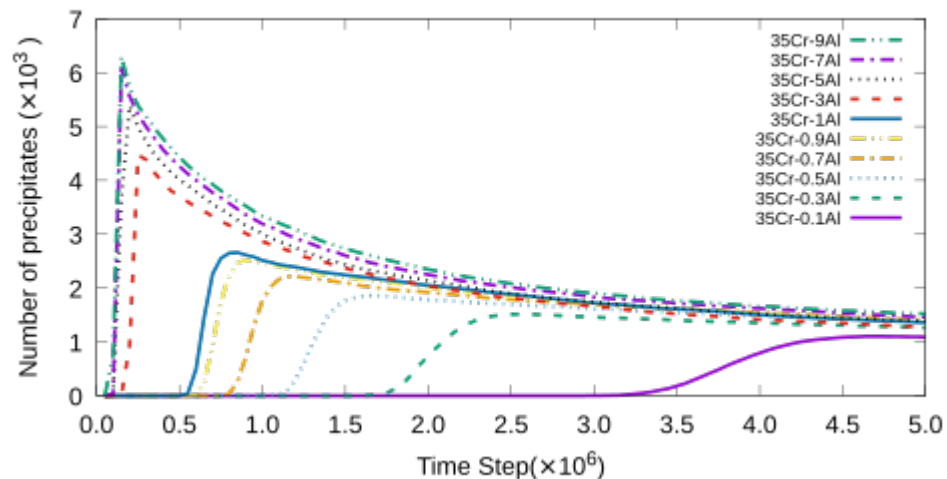
Plot of the Cr or Al concentration at  $t^* = 5.0 \times 10^6$  when the average Cr concentration was 35% and the average Al concentration was (a)(c) 1% (b)(d) 9%.

## Results

### 2D simulation result

#### As the Al concentration increase

- The phase separation occur early compared to low average Al concentration.
- The peak of the  $\alpha'$  phase number density increase.
- The number of the  $\alpha'$  phase precipitates decrease significantly after the peak when the high average Al concentration..



## Results

### 3D simulation result

- Tendency for the  $\alpha'$  phase forming an interconnected structure.

- In 2D simulation

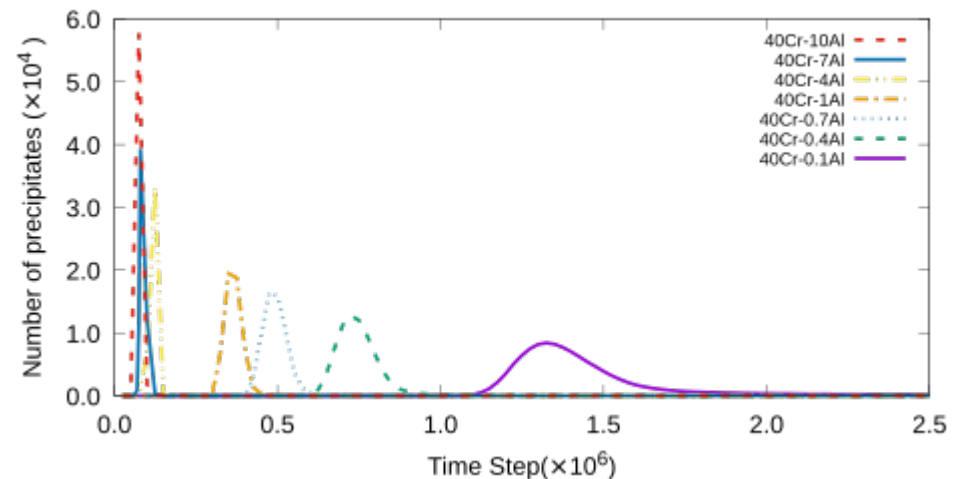
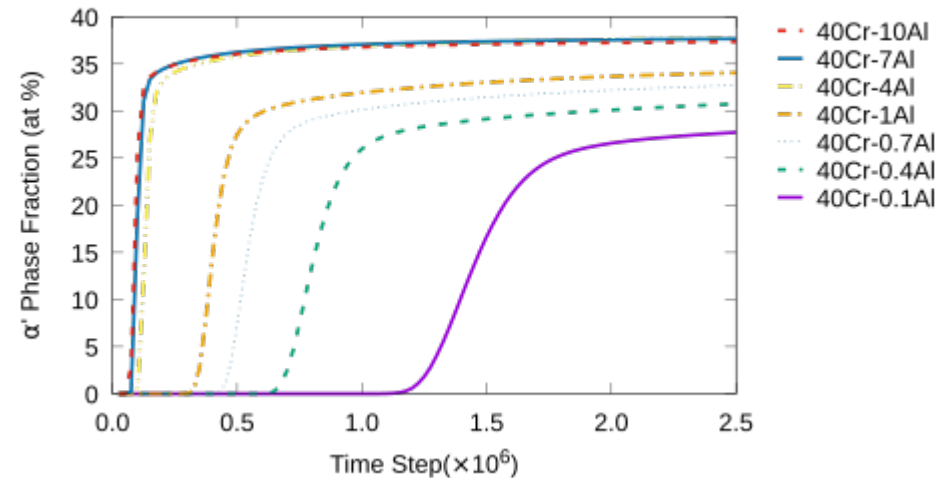
$$P_i^{2D} = 1.0 - (1 - f_{\alpha'})^4.$$

- In 3D simulation

$$P_i^{3D} = 1.0 - (1 - f_{\alpha'})^6.$$

$f_{\alpha'}$  : fraction of the  $\alpha'$  phase

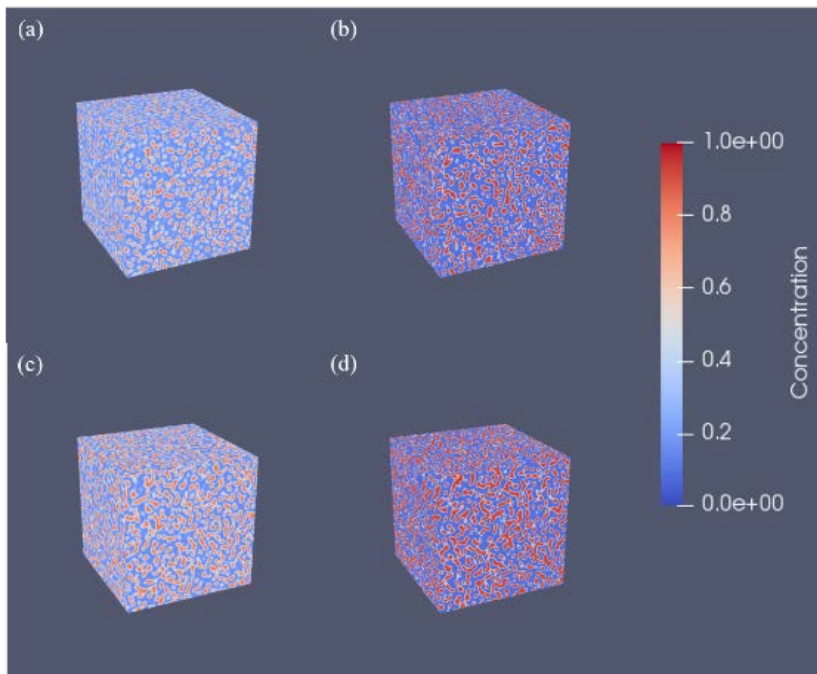
- The tendency of the 3D simulation to form interconnected structure is higher than that of the 2D simulation.



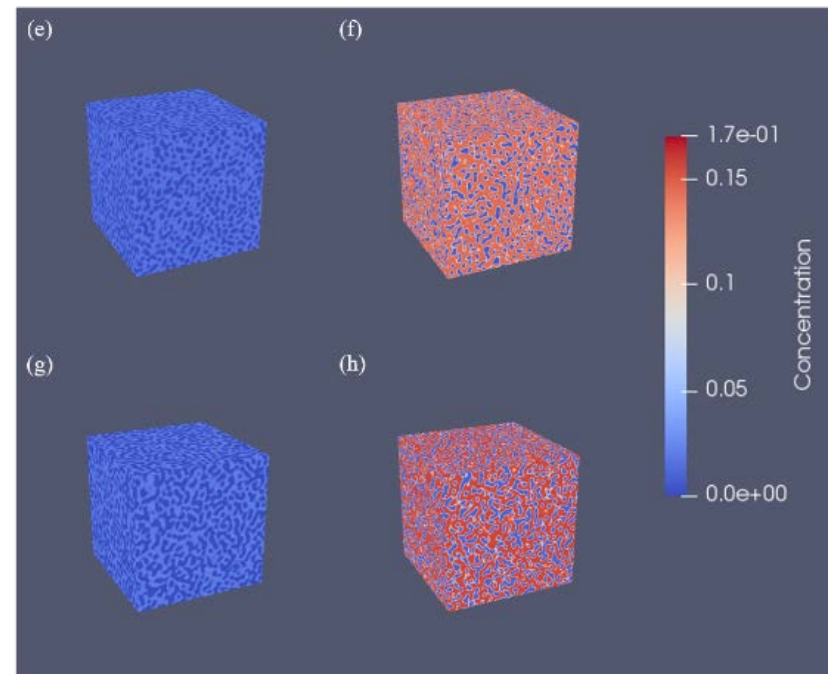
## Results



### 3D simulation result



Plot of the Cr concentration field at  $t^* = 2.5 \times 10^6$ .  
(a) 35Cr-1Al, (b) 35Cr-10Al, (c) 40Cr-1Al, (d) 40Cr-10Al.



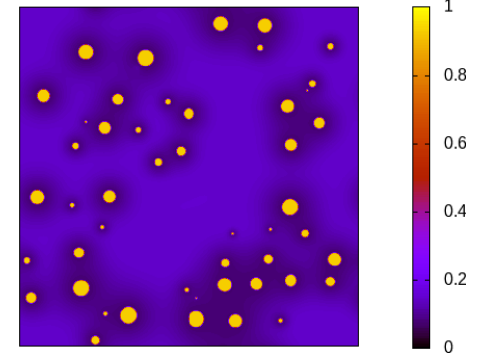
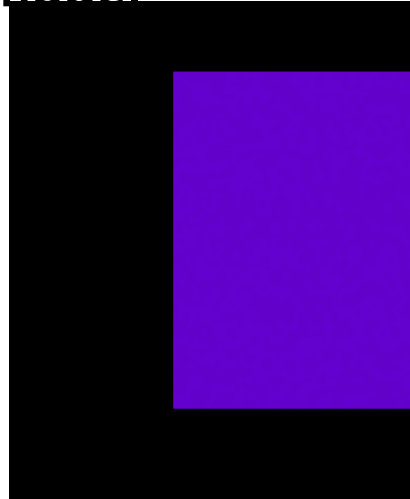
Plot of the Al concentration field at  $t^* = 2.5 \times 10^6$ .  
(e) 35Cr-1Al, (f) 35Cr-10Al, (g) 40Cr-1Al, (h) 40Cr-10Al.

## Future Work



### □ Incorporate nucleation model

- Classical nucleation theory.
- Poisson seeding algorithm



### □ Effect of neutron irradiation on the microstructural evolution of the Fe-Cr-Al alloy

- Radiation-enhanced diffusion (RED) model.
- Cascade mixing model.

## Conclusion



- The effect of Al concentration on the microstructural evolution of Fe-Cr-Al system was investigated by the phase-field model.
- We applied some methods that CALPHAD method, phase-field method, semi-implicit Fourier spectral method and GPU parallel computing scheme to simulate the microstructural evolution of Fe-Cr-Al alloy.
- An increase in the average Al concentration enhanced the initiation of phase separation, and the  $\alpha'$  phase fraction.
- At 35Cr% and 40Cr%, the formation of an interconnected structure of the  $\alpha'$  phase was observed in the 3D simulation, whereas the interconnected structure was not formed at the same chemical composition in 2D simulation.

## Acknowledgement



This work has supported by the National Research Foundation of Korea (NRF) grant funded by the Korea government (MSIT) (NRF-2018R1C1B5040669). This work was also supported by the “Human Resources Program in Energy Technology” of the Korea Institute of Energy Technology Evaluation and Planning (KETEP), granted financial resources from the Ministry of Trade, Industry & Energy, Republic of Korea (No. 20184030202170).



Ministry of Science and ICT



Ministry of Trade,  
Industry and Energy





Thank you